

# Bubble growth in non-evaporative drops of “Senko-hanabi”

Chihiro Inoue<sup>\*†</sup>, Yu-ichiro Izato<sup>\*\*</sup>, Atsumi Miyake<sup>\*\*</sup>, and Mitsuo KOSHI<sup>\*\*</sup>

<sup>\*</sup>Kyushu University, 744 Motoooka, Nishi-ku, Fukuoka-shi, Fukuoka, 819-0395 JAPAN

Phone: +81-92-802-3018

<sup>†</sup>Corresponding author: inoue.chihiro@aero.kyushu-u.ac.jp

<sup>\*\*</sup>Yokohama National University, 79-5 Tokiwadai, Hodogaya-ku, Yokohama-shi, Kanagawa, 240-8501 Japan

Received: November 14, 2017 Accepted: October 18, 2018

## Abstract

The traditional hand-held Japanese sparkler, Senko-hanabi, has been popular in Japan since the Edo period. The branching sparks, akin to pine-needles, are in fact the drops of a melt of potassium compounds accompanying their successive fragmentation with ever smaller droplets. This unique fragmentation cascade is self-sustained by the continuous heat from an exothermic surface reaction on the drop, in which internal nucleation growing as a bubble leads to it bursting at each step of cascade. In the present study, the drops of Senko-hanabi are found to be non-evaporative due to their low saturated vapor pressure. Then, the internal bubble radius is calculated. The bubble radius grows in proportion to the square root of the product of time and thermal diffusivity, which provides a direct evidence the thermal diffusion as the rate-controlling process. The thermal analysis indicates CO<sub>2</sub> as the main component of the bubble, however, the gas production mechanism is still an open question.

**Keywords:** sparkler, Senko-hanabi, bursting drop, bubble dynamics, visualization, thermal analysis

## 1. Introduction

Fireworks are popular all over the world. From the Edo period (1603–1868) in Japan, one of the most popular hand-held fireworks has been the Senko-hanabi (Figure 1). These are composed of a so-called “black powder”, a mixture of charcoal C, sulfur S, and potassium nitrate KNO<sub>3</sub>, in relative proportions of 15%, 25%, and 60% by weight, respectively, simply wrapped in a twisted paper. The firework is in the form of a 15-cm-long thin paper string, with the black powder at one end. One holds the paper string at its top end and ignites the lower end, upon which a red hot globule is formed and sparks are emitted. No metal powders are contained, and therefore, the sparks become luminous by black body radiation, creating a distinct fragile beauty.

More than a century ago, Denisse<sup>2)</sup> sketched the firework introduced from Japan and posed questions regarding the processes inside the globule that result in such astonishing spark behavior. Later, Terada<sup>3)</sup> was interested in the physical and chemical phenomena that occurred. Nakaya and Sekiguchi<sup>4)</sup> studied the Senko-



Figure 1 Senko-hanabi<sup>1)</sup>.

(At the bottom end of the paper string, a globule is formed, from which sparks are emitted.)

hanabi and mentioned the importance of the exothermic reaction of ambient oxygen with carbon within the black powder. Shimizu<sup>5)</sup> noticed that potassium compounds were essential reaction products for the spark generation.

He also pointed out that the charcoal of tung and pine was suitable for the firework, whereas carbon black produced no sparks. Maeda and his high school students<sup>6)</sup> were the first to carry out chemical analyses. They identified the existence of potassium sulfide ( $K_2S$ ), potassium carbonate ( $K_2CO_3$ ), potassium sulfate ( $K_2SO_4$ ), and C without the oxidizer of  $KNO_3$ . This important result confirms that Senko-hanabi is no longer an explosive after ignition, as previously pointed out by Nakaya<sup>4)</sup>. In spite of a long history, however, the physical and chemical processes at play in these fireworks have remained elusive. Recently, Inoue *et al.*<sup>1), 7), 8)</sup> reported the detailed sequence of events by a comprehensive strategy that involved high-speed photography, two-wavelength pyrometry, thermal analysis, theoretical modeling, and statistics. Inoue *et al.* evidenced that the pine-needle-like sparks are in fact the trajectories of drops in the melt of potassium compounds accompanying their successive fragmentation with ever smaller droplets. At each drop fragmentation step, an internal bubble inflates leading to the rapid expansion of drop, and to its rupture in the end. Therefore, the bubble dynamics is essential for the drop fragmentation as well as for the spark ramifications.

As a similar phenomenon, the bursting of evaporative drops has been well known called as micro-explosion and puffing<sup>9)</sup>. In contrast, the potassium compounds inside the Senko-hanabi drops are non-evaporative. In the present study, we investigate the time variant drop size of Senko-hanabi to verify the non-evaporative feature, and directly calculate the bubble dynamics inside the drops to understand the rate controlling step. We also try to suggest a chemical mechanism of nucleation and bubble growth.

## 2. Experimental apparatus

The sparklers used in this study were produced by the Tsutsui-Tokimasa toy fireworks factory<sup>10)</sup>. A monochrome high-speed video camera, Photron SA-X, was employed to record instantaneous backlit images. The typical frame rate and shutter speed were set at 10,000 fps and 1/100,000 s, respectively. The image resolution was  $1024 \times 1024$  pixels. We measured the time variant drop size as the area equivalent radius.

To identify the gases produced inside the drops, we employed thermogravimetry-differential thermal analysis (TG-DTA) instrumentation interfaced with a mass spectrometer (MS). A Rigaku TG8120 instrument was used for TG-DTA, in conjunction with a Shimadzu GC-2010 instrument for MS. The TG-DTA-MS data were acquired simultaneously to assess samples from a part of the globule, as well as various standard potassium compounds. In these measurements, approximately 3 mg of the samples were placed in aluminum pans and heated from 300 to 1500 K at  $10 \text{ K min}^{-1}$  under helium. The gases evolved during each test were sent to the MS by the helium gas flow. The MS was operated in the electron impact ionization mode.

## 3. Results and discussions

### 3.1 Time variant drop size

Instantaneous shadow images are overlapped to yield a time-integrated image in Figure 2. Obviously, the sparks originating from the globule are trajectories of the flying drops, which are emitted by bubbles bursting on the globule<sup>7), 8)</sup>. The drops eventually burst giving rise to several daughter drops. From the clear images, we measured the drop radius ( $R$ ) from  $t = 0$  (ejected from the globule) to the instant at which it bursts (Figure 3). The drop size remains constant for most of its lifetime ( $R = R_0$ ) and suddenly expands, reaching the maximum size of  $R = R^*$  and bursts. Here, internal nucleation growing to a bubble leads to the drop expansion.

Figure 4(a) shows the time variant size of several drops from  $t = 0$  to just before the expansion. The size is almost constant independent of the initial size. In Figure 4 (b), each radius is normalized by the corresponding value of  $R_0$  and plotted against normalized time. The decrement of  $R/R_0$  is less than 10%. The trend does not coincide with the change of evaporative drops inducing conventional micro-explosion as the burning rate constant ( $\text{mm}^2 \text{ s}^{-1}$ ) of approximately unity (dashed line, so-called  $d^2$ -law)<sup>9)</sup>. The saturated vapor pressure of  $K_2CO_3$ ,  $P(K_2CO_3)$ , at temperature of  $T$ , is given as<sup>11)</sup>:

$$\ln P(K_2CO_3) = -37691.96/T + 17.30 \quad (693 \text{ K} \leq T \leq 1173 \text{ K})$$

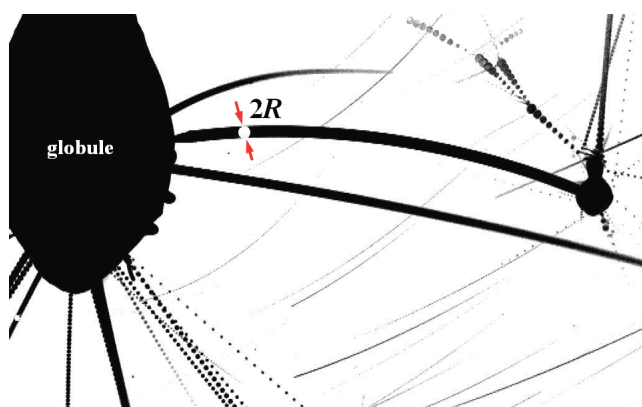


Figure 2 A flying drop with radius  $R$ . (Black lines are the trajectories of drops that are seen as sparks.)

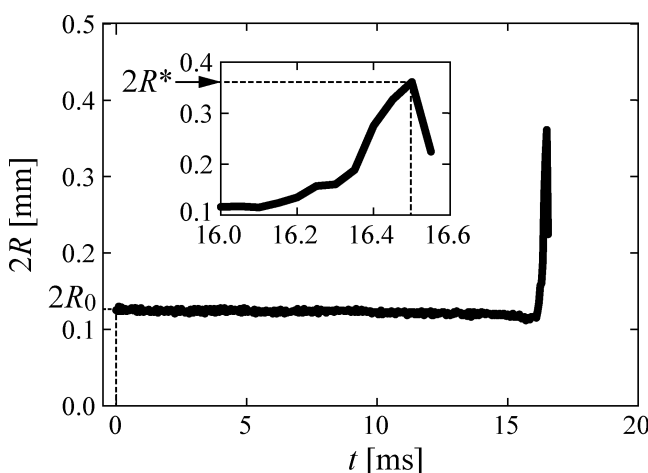
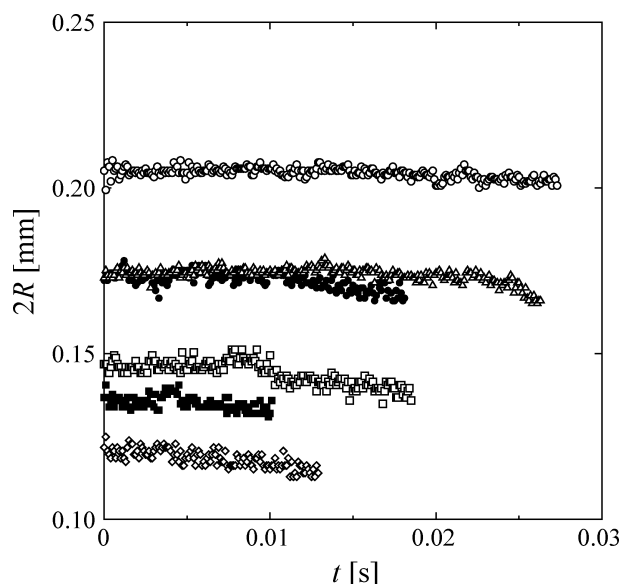
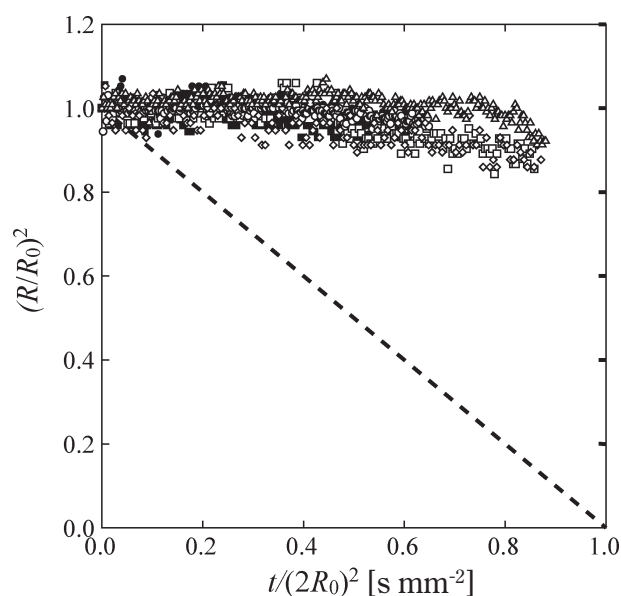


Figure 3 Time variant drop radius  $R$ . (Initial radius is  $R_0$ , and the maximum size is  $R^*$ .)


 (a) Time variant  $R$  before expansion


(b) Normalized radius

(Dashed line indicates the trend of typical evaporative drops.)

**Figure 4** Time variant drop radius of  $R$ .

$$= -34268.21/T + 17.06 - 0.00233T$$

$$(1173 \text{ K} \leq T \leq 3000 \text{ K})$$

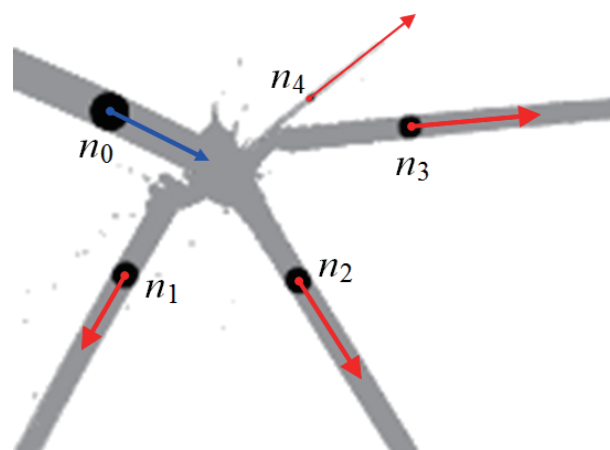
 and for  $\text{K}_2\text{SO}_4$ <sup>11)</sup>:

$$\ln P(\text{K}_2\text{SO}_4) = -36487.3/T + 16.06 \quad (857 \text{ K} \leq T \leq 1342 \text{ K})$$

$$= -26462.6/T + 8.786 \quad (1342 \text{ K} \leq T \leq 3000 \text{ K}).$$

Even at  $T = 1300 \text{ K}$  corresponding to the highest temperature of Senko-hanabi<sup>1)</sup>,  $P(\text{K}_2\text{CO}_3) = 4.4 \times 10^{-6} \text{ bar}$ , and  $P(\text{K}_2\text{SO}_4) = 6.1 \times 10^{-6} \text{ bar}$ , which are quite low values. Therefore, the drops of Senko-hanabi are non-evaporative, consistent with the low saturated vapor pressure of the potassium compounds in the drops.

As depicted in Figure 5, a drop bursts and produces several daughters, whose size and volume are summarized in Table 1. Since the total volume before and after the bursting event is maintained, the drop size decreases only by fragmentation, without evaporation.


**Figure 5** Trajectory lines of drops before and after bursting. (The drop of  $n_0$  fragments producing daughters of  $n_1, n_2, n_3, n_4$ )

**Table 1** Size of drops in Figure 5

	name	$2R$ [mm]	vol. [ $10^{-5} \text{ mm}^3$ ]
Before burst	$n_0$	0.18	303
After burst	$n_1$	0.13	109
	$n_2$	0.13	104
	$n_3$	0.12	82
	$n_4$	0.05	5

(Total volume of the daughters is  $3 \times 10^{-3} \text{ mm}^3$ , which is almost same as the volume of  $n_0$ .)

### 3.2 Bubble dynamics

Assuming that one bubble exists inside the non-evaporative drop, as shown in Figure 6, the radius  $b$  is calculated from the measured values of  $R$  and  $R_0$ .

$$b = (R^3 - R_0^3)^{1/3} \quad (1)$$

It is natural that  $b = 0$  at  $t = 0 \text{ s}$ , and  $b$  increases after the pre-heating process, as follows<sup>1)</sup>.

$$t \sim R_0^2/\chi \quad (2)$$

Here, the thermal diffusivity is denoted by  $\chi \sim 10^{-6} \text{ m}^2 \text{ s}^{-1}$ . Let us define the time for a bubble to inflate as

$$\hat{t} = t - R_0^2/\chi \quad (3)$$

When the gas production is rate-controlled by thermal diffusion around the surface of the bubble,  $b$  increases according to the Plesset and Zwick equation<sup>12)</sup>.

$$b \sim \sqrt{\chi \cdot \hat{t}} \quad (4)$$

As evidenced by Figure 6, the experimental results satisfy Equation (4). Thermal diffusion inside the drops takes much longer time than gas production process. Figure 6 also indicates that gas production is an endothermic process (but not evaporation), and the single bubble inflates inside a drop. Since the molecular diffusion coefficient,  $D \sim 10^{-8} \text{ m}^2 \text{ s}^{-1}$ , is much smaller than  $\chi$ , ambient oxygen and also produced gas on the drop surface cannot reach the bubble surface and do not influence bubble growth.

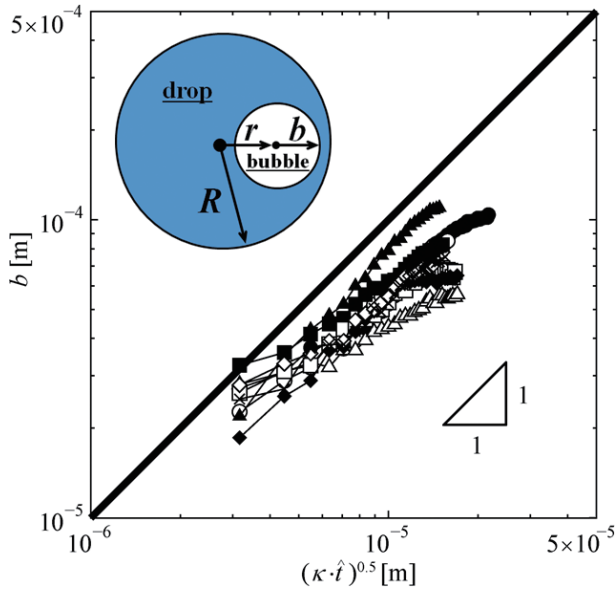
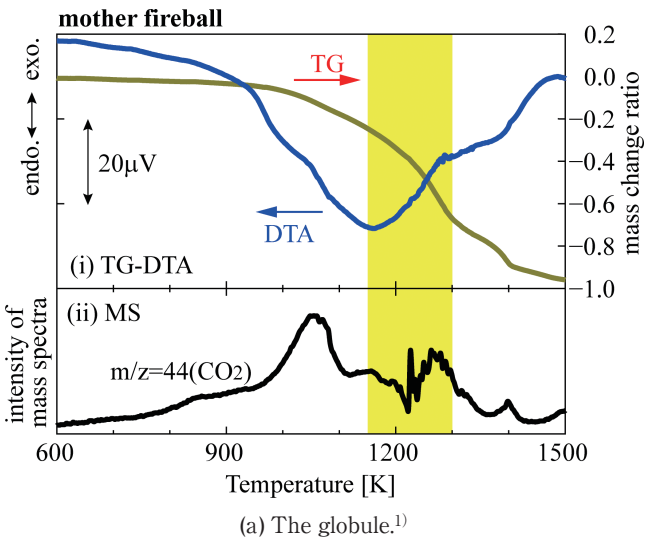


**Figure 6** Growing bubble radius inside drops. (Bold line indicates  $b = 10\sqrt{\kappa \cdot \hat{t}}$  and all experimental results (symbols) consistently satisfy  $b \sim \sqrt{\kappa \cdot \hat{t}}$ .)

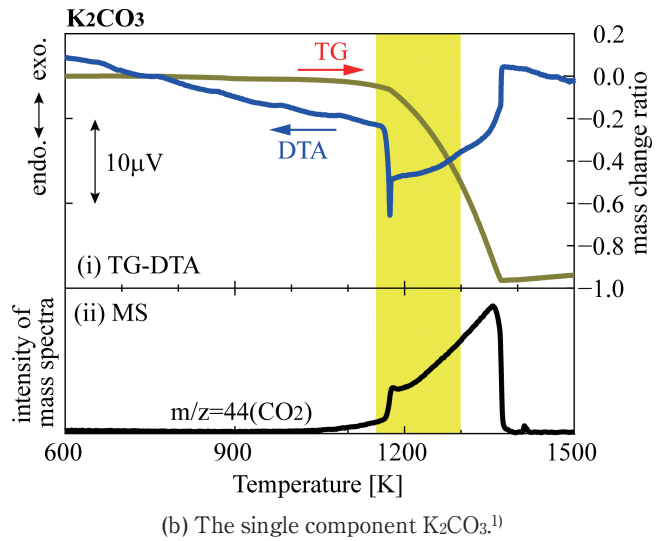
### 3.3 Thermal analysis

Thermal analysis was conducted in order to investigate the gas production mechanism inside the inflating drops. We used the components constitutive of the globule, and a single component, namely  $K_2CO_3$ ,  $K_2S$ , and  $K_2SO_4$ , in four different cases. It is reasonable to assume that the components of the globule are consistent with those of the drops. The temperature range was 1150–1300 K, corresponding with the drop temperature in Senkohanabi.<sup>1)</sup>

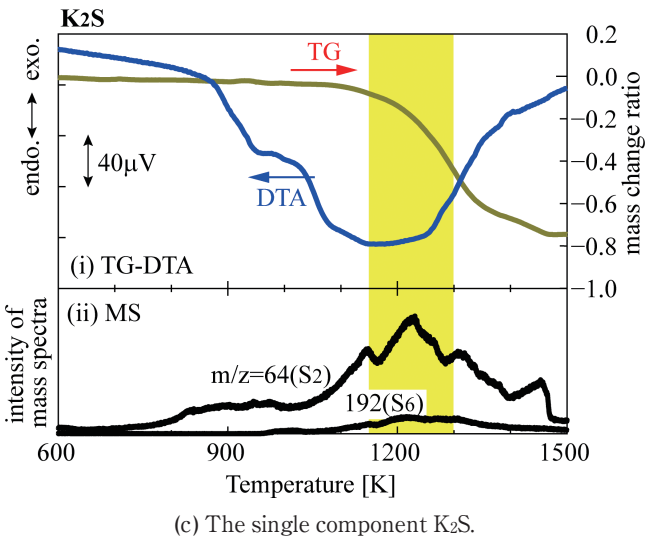
Figure 7(a) presents the TG-DTA-MS results obtained from a portion of a globule. While scanning over the temperature range of drops, the mass variation indicated by TG is seen to decrease steeply as the result of endothermic gas production, and the main gaseous product is  $CO_2$ . The result for the single component  $K_2CO_3$  in Figure 7(b) indicates that the endothermic thermal decomposition generates  $CO_2$  at temperatures above its melting point of 1164 K. However, the saturated vapor pressure of  $K_2CO_3$  is quite low as discussed previously, it is not reasonable to conclude that thermal decomposition of  $K_2CO_3$  produce sufficient amount of  $CO_2$  inside the drops. We were also able to confirm that another component,



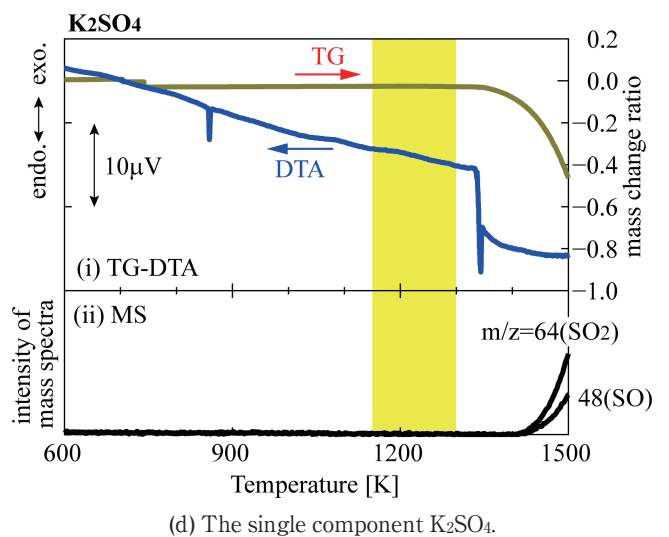
(a) The globule.<sup>1)</sup>



(b) The single component  $K_2CO_3$ .<sup>1)</sup>



(c) The single component  $K_2S$ .



(d) The single component  $K_2SO_4$ .

**Figure 7** Results of thermal analyses. (The yellow band (1150 to 1300 K) indicates the drop temperature.)

$K_2S$ , produces gaseous  $S_2-S_6$  in this temperature range (Figure 7(c)), although in much lower amounts compared to the  $CO_2$  from  $K_2CO_3$ .  $K_2SO_4$  did not produce any gases over this temperature range (Figure 7(d)). Since the boiling point of sulfur S is 718 K, any gas production from sulfur would be complete and thus does not affect the bubble growth.

Recently, Seki and his colleagues<sup>13)</sup> developed a product similar to Senko-hanabi using  $K_2CO_3$  instead of  $KNO_3$ , for safety reasons. The “oxidizer free” Senko-hanabi does not include an oxidizer. Surprisingly, it produces branching sparks similar to the original Senko-hanabi after sufficient heating. In contrast, the case using  $K_2SO_4$  instead of  $KNO_3$  does not emit sparks. We believe this is an evidence for the importance of  $K_2CO_3$  for spark ramifications. However, for a more detailed understanding of the chemical aspects, further analysis is needed.

#### 4. Conclusions

We directly investigated the bubble growth rate leading to drop expansion and fragmentation in the non-evaporative drops of the Senko-hanabi by high-speed image analyses. We also investigated the chemical mechanism of feeding gas to the bubble. The conclusions are summarized as follows.

- (1) The sparks are the trajectories of non-evaporative flying drops, whose time variant diameter does not follow  $d^2$ -law.
- (2) Inside the non-evaporative drops, nucleation occurs and the single bubble inflates rate-controlled by thermal diffusion.
- (3) The main gas component is  $CO_2$ , however, the

production mechanism is not yet clarified.

#### Acknowledgement

This work was partially supported by KAKENHI (17H00844).

#### References

- 1) C. Inoue, Y. Izato, A. Miyake, and E. Villermaux, *Phys. Rev. Lett.*, 118, 074502 (2017).
- 2) A. Denisse, *Feux D'Artifice* (1882).
- 3) T. Terada, *Senko-hanabi (1927)*. (in Japanese).
- 4) U. Nakaya and Y. Sekiguchi, *Bulletin of the Institute of Physical and Chemical Research*, 6, 1083–1103 (1927). (in Japanese).
- 5) T. Shimizu, *Journal of the Industrial Explosives Society (Sci. Tech. Energetic Materials)*, 18, 359–369 (1957). (in Japanese).
- 6) A. Maeda, *Research Report on Senko-hanabi* (1962). (in Japanese).
- 7) C. Inoue, M. Koshi, H. Terashima, T. Himeno, and T. Watanabe, *Sci. Tech. Energetic Materials*, 74, 106–111 (2013).
- 8) C. Inoue, M. Koshi, T. Himeno, and T. Watanabe, *Sci. Tech. Energetic Materials*, 77, 51–58 (2016).
- 9) T. Kadota and H. Yamasaki, *Progress in Energy and Combustion Science*, 28 385–404(2002).
- 10) Tsutsui Tokimasa Fireworks, <http://tsutsuitokimasa.jp>
- 11) M. Koshi, *Sci. Tech. of Energetic Materials*, 79, 59–69 (2018).
- 12) M. S. Plesset and S. A. Zwick, *J. Appl. Phys.*, 25, 493–500 (1954).
- 13) T. Seki, *A Non-Explosive Senko-hanabi* (2017). (in Japanese). <http://www.kagakunosaiten.jp/convention/pdf/2017/022.pdf>